Science Front Publishers *Journal for Foundations and Applications of Physics*, **vol. 11, No. 1 (2024)**
(sciencefront.org) **ISSN 2394-3688**

Effect of CIGS Layer Thickness and Bandgap on the Efficiency of Thin-Film Copper Indium Gallium Selenide (CIGS) Solar Cells Using GPVDM

Hassan Abdulsalam* and Fatima Musa Lariski

Department of Physics, Faculty of Science
Yobe State University, P.M.B 1144, Damaturu, Yobe State, Nigeria
**Corresponding author E-mail*: hassanklinsmann@gmail.com
(Received 06 November 2023, Accepted 11 February 2024, Published 27 February 2024)

Abstract
This study explores how CIGS absorber layer thickness and bandgap influenced the efficiency of Copper Indium Gallium Selenide (CIGS) thin-film solar cells through simulations carried out using the General-Purpose Photovoltaic Device Model (GPVDM). The unique properties of CIGS, including its tunable energy bandgap, are highlighted for optimal alignment with the solar spectrum. Through sets of simulation, optimal values are determined for thickness and bandgap. Results indicate an optimal thickness range (1.2 to 1.3 µm), striking a balance between absorption and recombination losses. Furthermore, an optimal bandgap range (between 1.261 eV and 1.596 eV) was identified, aligning photon absorption and energy losses for maximal efficiency. These findings underscore the nuanced optimization required for effective solar cell design, with implications for the advancement of renewable energy technologies.

***Keywords*:** CIGS solar cells; Absorber layer thickness; Bandgap; Photovoltaic efficiency; Thin-

1. INTRODUCTION

The first solar cell based on copper indium diselenide ($CuInSe_2$) was introduced by Bell Telephone Laboratories in 1974, the initial solar cell achieved a conversion efficiency of 6%. Building upon this progress, a CdS/$CuInSe_2$ solar cell was developed in 1982, which improved the conversion efficiency to 10% [1]. As researchers continued to refine the technology, they began substituting gallium for some of the indium in $CuInSe_2$, resulting in the creation of copper indium gallium diselenide (CIGS). This new material had a wider optical bandgap compared to pure CIS, leading to an increase in the open-circuit voltage of the solar cell. Copper Indium Gallium Selenide (CIGS) solar cells, belong to the category of thin-film solar cells [2], these cells are produced by applying a thin layer of a solution containing copper indium gallium selenide onto a substrate made of glass or plastic, electrodes are positioned on the front and back of the cell to capture the generated current.

The potential of CIGS solar cells lies in their ability to lower the production costs of photovoltaic devices [3]. The highest lab efficiency in thin film technology is 23.4% for CIGS and 21.0% for CdTe solar cells [4]. Over the years, there were successive improvements in the efficiency of $CdS/Cu(In,Ga)Se_2$ solar cells. The efficiency increased to 15% in 1993, then to 17.7% in 1996, followed by a further advancement to 19.2% in 2003 [5]. Subsequently, there were additional gains, with efficiency reaching 19.9% in 2008 [6]. As the performance, consistency, and dependability of CIGS products advance, this technology could significantly increase its market share. The CIGS layer serves as solar the harvested, within this layer, sunlight is absorbed, initiating the photovoltaic effect which generates an electron-hole pair, the main goal is to efficiently capture the electron before it encounters any obstacles and gets re-absorbed, a phenomenon known as recombination.

Copper indium gallium diselenide (CIGS) stands as a semiconductor substance in the $I\text{-}III\text{-}VI_2$ category, comprising copper, indium, gallium, and selenium elements [7], CIGS constitutes a firm amalgamation of copper indium selenide (often denoted as "CIS") and copper gallium selenide. Its chemical formula is $CuIn_{1-x}GaxSe_2$, where the parameter x has a range of values from 0 (indicating pure copper indium selenide) to 1 (representing pure copper gallium selenide). CIGS exhibits a tetrahedral bonded structure and follows the chalcopyrite crystal configuration. CIGS in its polycrystalline form has become widely favored as a leading material for photovoltaic applications [8]. The key characteristic that makes the CIGS compound appealing is its capacity to adjust its energy band gap within the range of 1.01 eV to 1.68 eV through the manipulation of the Ga fraction, this enables it to closely align with the solar spectrum for optimal performance [9]. Band-gap engineering geared to controlling the spatial distribution of the Ga content in the absorber layer can lead to enhancing the overall performance of CIGS cells [10].

The thickness of the CIGS absorber layer has a significant impact on the light absorption within a thin film CIGS solar cell. In the standard configuration, the CIGS absorber layer typically ranges from 1.5 to 2 μm [11]. The absorption efficiency of the bulk CIGS layer decreases progressively with increasing wavelength. This means that as wavelength becomes longer, the CIGS layer becomes more translucent, resulting in reduced absorption. This implies that in order to achieve significant light absorption, the CIGS layer needs to be sufficiently thick to ensure that it remains optically "opaque" across the entire relevant spectrum. When reducing the CIGS layer thickness from 2 μm to 500 nm, significant optical losses occur within the wavelength range of 700 to 1100 nm. This range corresponds to wavelengths where the CIGS layer can only partially absorb light. Much of the light that is not absorbed in the CIGS layer passes through and gets absorbed in the Mo (back contact) layer [12]. The thickness of the CIGS absorber layer plays a crucial role in determining the light absorption characteristics of thin film CIGS solar cells [13]. Proper thickness optimization is essential to ensure effective light absorption across the desired spectrum and to prevent undesirable optical losses[12]. This study examined how the efficiency of CIGS solar cells is influenced by factors such as CIGS thickness and bandgap. The investigation utilized the General-Purpose Photovoltaic Device Model (GPVDM).

2. CURRENT DENSITY-VOLTAGE (J-V) CHARACTERISTICS AND PARAMETERS OF A SOLAR CELL

The main electrical parameters of a solar cell can be analyzed by studying its current-voltage characteristics curve. Some of these parameters are: short circuit current (I_{sc}), open- circuit voltage (V_{oc}), maximum power point voltage (V_{mp}), maximum power point current (I_{mp}), maximum power point (MPP), fill factor (FF) and power conversion efficiency (η).

2.1 The Short Circuit Current-Density

The short circuit current- density (J_{sc})is the current that flows through the external circuit when the electrodes of the solar cell are short circuited, it depends on the surface area of the solar cell. The short-circuit current of a solar cell depends on the photon flux incident on the solar cell, which is determined by the spectrum of the incident light. For standard solar cell measurements, the spectrum is standardized to the AM1.5 spectrum. The maximum current that the solar cell can deliver strongly depends on the optical properties of the solar cell, such as absorption in the absorber layer and reflection[14].

2.2 The Open- Circuit Voltage

The open-circuit voltage (V_{oc}) is the voltage at which no current flows through the external circuit. It is the maximum voltage that a solar cell can deliver. V_{oc} corresponds to the forward bias voltage, at which the dark current density compensates the photocurrent density. V_{oc} depends on the photo-generated current density assuming that the net current is zero.

$$V_{oc} = \frac{k_B T}{q} \ ln\left(\frac{J_L}{J_o} + 1\right) \approx \frac{k_B T}{q} \ ln\left(\frac{J_L}{J_o}\right) \quad (1),$$

The approximation is justified because of $J_L \gg J_o$.

where k_B is the Boltzmann constant, T is the temperature, q is the elementary electric charge, J_L is the light-induced current density, and J_o is the diode saturation current density. V_{oc} depends on the diode saturation current density of the solar cell and light-induced current density. The light-induced current density depends on the recombination in the solar cell.

2.3 Maximum Power Point Voltage, Maximum Power Point Current and Maximum Power Point

Maximum power point voltage (V_{mp}) and Maximum Power Point Current (I_{mp}) are the voltage and current respectively when the power output is the greatest. The maximum power point (MPP) is the point at which the product of the current and voltage equal the greatest value.

2.4 The Fill Factor (FF)

The fill factor FF is the ratio of the maximum power generated P_{max} by a solar cell and the product of V_{oc} and J_{sc}. [15].

$$FF = \frac{P_{max}}{V_{oc} \times J_{sc}} \quad (2)$$

The conversion efficiency is calculated as the ratio between the maximum generated power and the incident power. Solar cells parameters are measured under the Standard Test Conditions(STC), where the incident light is described by the AM1.5 spectrum and has an irradiance of 1000 W/m^2[16].

$$\eta = \frac{V_{oc} \times J_{sc} \times FF}{P_{in}} = \frac{P_{max}}{P_{in}} \quad (3)$$

where P_{in} is the input power, for efficiency calculations input power is 1 kW/m^2.

3 METHODOLOGY

This section outlines the methodology employed in this study; The General-purpose Photovoltaic Device Model (GPVDM) was used in simulating the CIGS solar cell. The study involves two sets of simulations: one focused on varying the thickness of CIGS absorber layer, and the other on varying the bandgap of the CIGS material.

3.1 General-purpose Photovoltaic Device Model

General-purpose Photovoltaic Device Model (GPVDM). GPVDM is a free general-purpose tool for the simulation of light-harvesting devices. The model solves both electrons and holes drift-diffusion, and carrier continuity equations in position space to describe the movement of charge within the device. The model also solves Poisson's equation to calculate the internal electrostatic potential. Recombination and carrier trapping are described within the model using Shockley-Read-Hall (SRH) formalism, the distribution of trap states can be arbitrarily defined. The software manual contains a more detailed model description[17]. The software gives outputs that contain the solar cell parameters (open-circuit voltage Voc, short-circuit current density Jsc, fill factor FF, and efficiency η among others) and Current-Voltage (I-V) characteristic curves[18].

3.2 Simulations

This study involves of two sets simulations, the first involves varying the thickness of the CIGS layer, while the second involves the varying of the bandgap of the CIGS layer.

3.2.1 Varying CIGS Absorber Layer Thickness

In the first set of simulations, the thickness of the CIGS absorber layer was varied from 1.0 to 2.0 µm in a step of 0.1 µm. The simulations use the default values for electrical parameters, doping levels, and parasitic components.

3.2.2 Varying CIGS Absorber Layer Bandgap

The optimal absorber layer thickness determined from the first set of simulations was retained for the second set of simulations. Here, the bandgap of the CIGS material was varied from of 1.01 to 1.68 eV in a step of 0.08 eV. Similarly, the default values were maintained for other electrical parameters, doping levels, and parasitic components.

4 RESULTS AND DISCUSSION

The J-V characteristics curves obtained for the first and second sets of simulations are shown in figures 1 and 2 respectively. The Solar cell parameters obtained from figures 1 and 2 are presented in Tables 1 and 2, respectively. The graphs depicting efficiency against thickness and bandgap are presented in Figures 3 and 4, respectively.

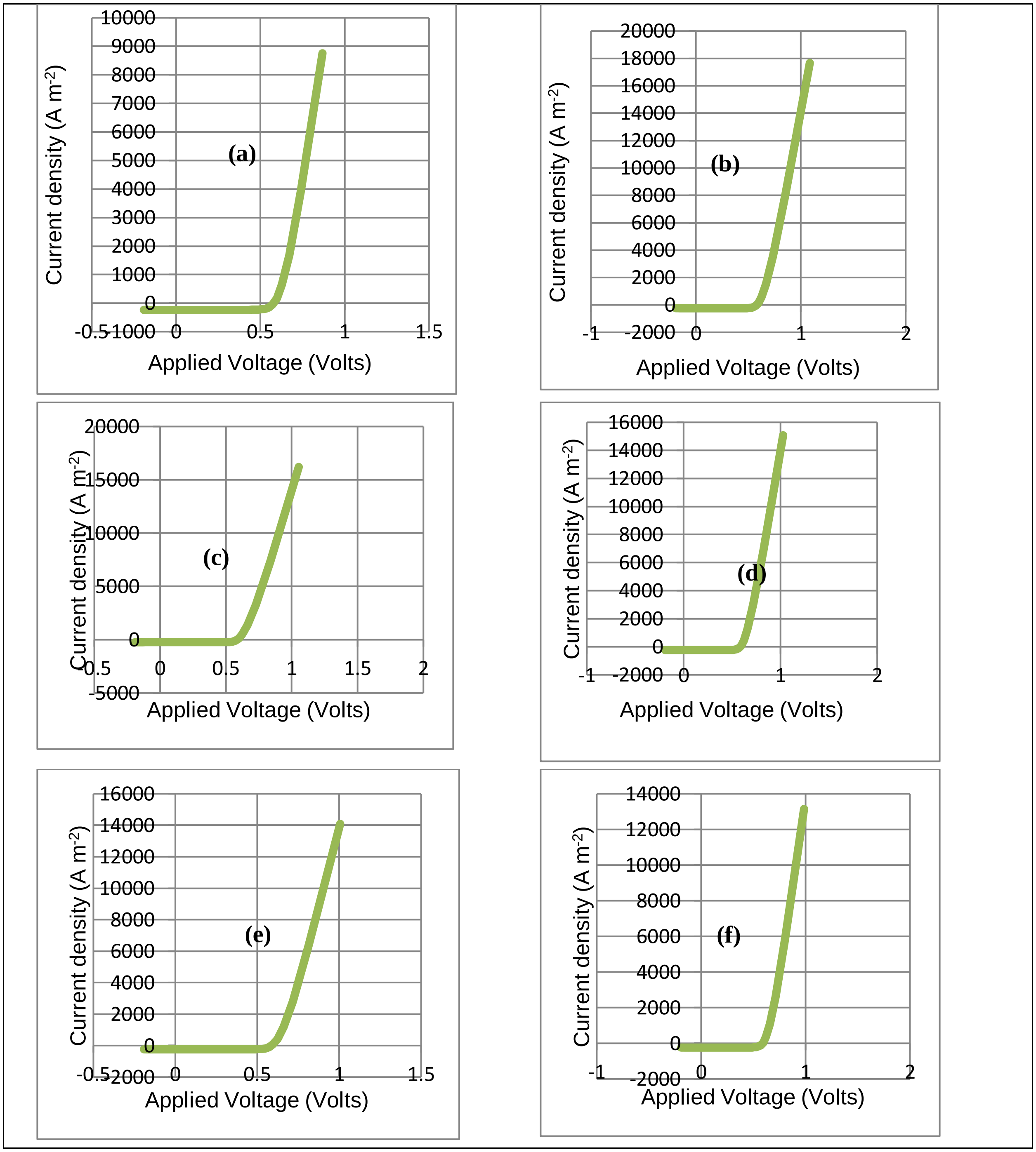

***Figure 1A** Current density - Applied voltage Curves for First set of Simulations:* $(a)\,Thickness = 1.0\ \mu m$, $(b)\,Thickness = 1.1\ \mu m$, $(c)\,Thickness = 1.2\ \mu m$, $(d)\,Thickness = 1.3\ \mu m$, $(e)\,Thickness = 1.4\ \mu m$ *and* $(f)\,Thickness = 1.5\ \mu m$

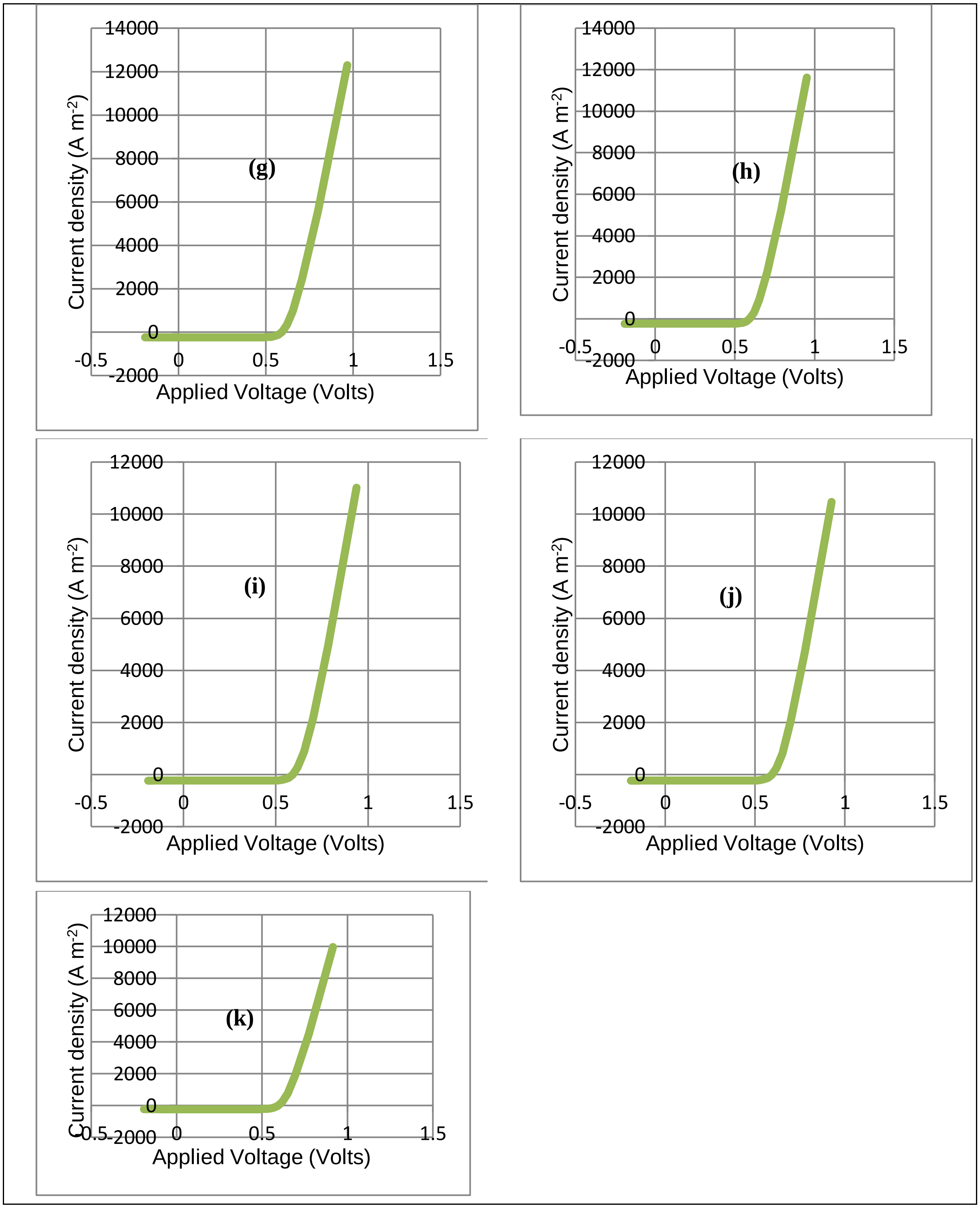

Figure 1B *Current density - Applied voltage Curves for First set of Simulations:* $(g)\ Thickness = 1.6\ \mu m$, $(h)\ Thickness = 1.7\ \mu m$, $(i)\ Thickness = 1.8\ \mu m$, $(j)\ Thickness = 1.9\ \mu m$, *and* $(k)\ Thickness = 2.0\ \mu m$

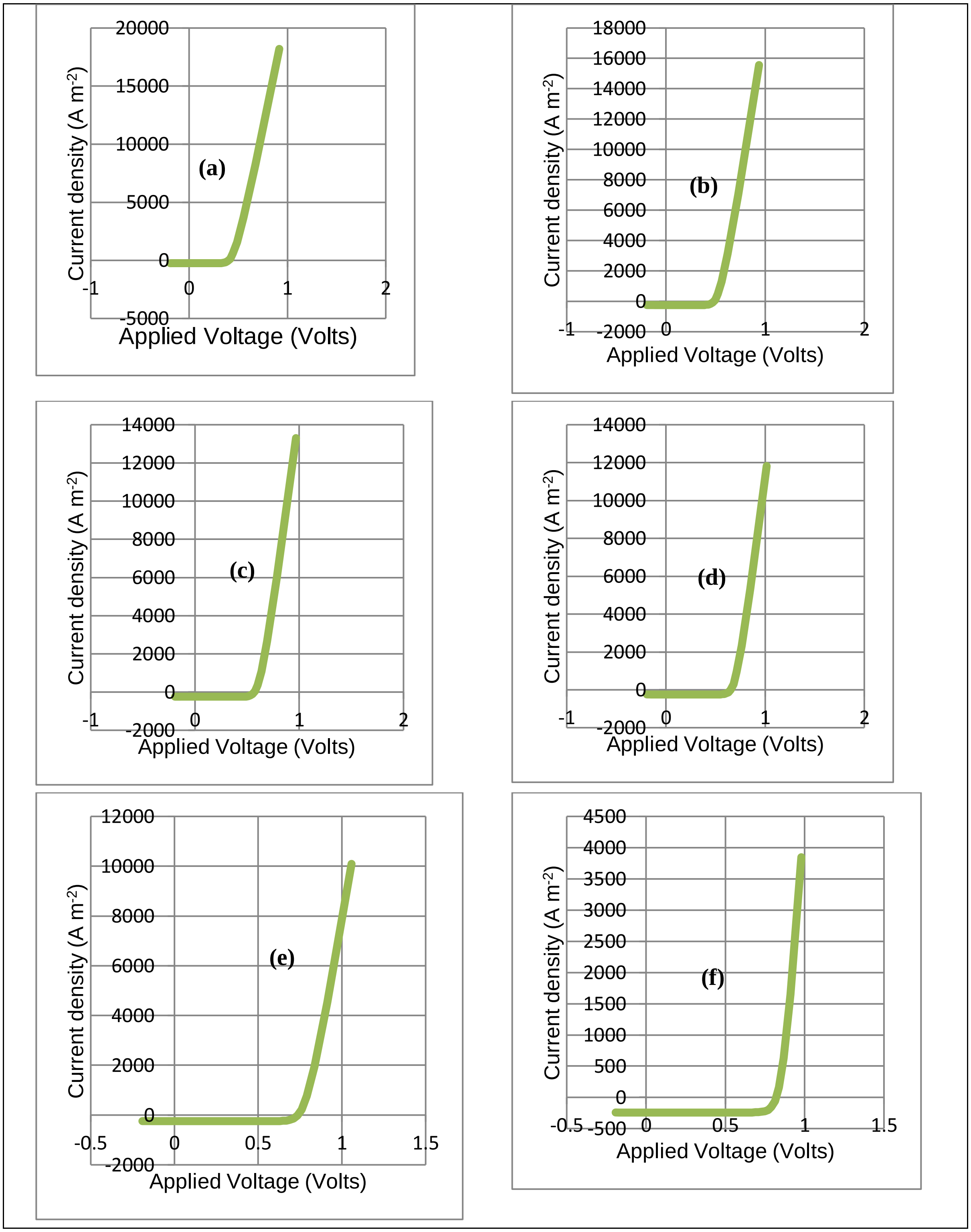

Figure 2A *Current density - Applied voltage Curves for second set of Simulations: (a)* $Bandgap = 1.01\ eV$, *(b)* $Bandgap = 1.09\ eV$, *(c)* $Bandgap = 1.18\ eV$, *(d)* $Bandgap = 1.26\ eV$, *(e)* $Bandgap = 1.35\ eV$ *and (f)* $Bandgap = 1.43\ eV$

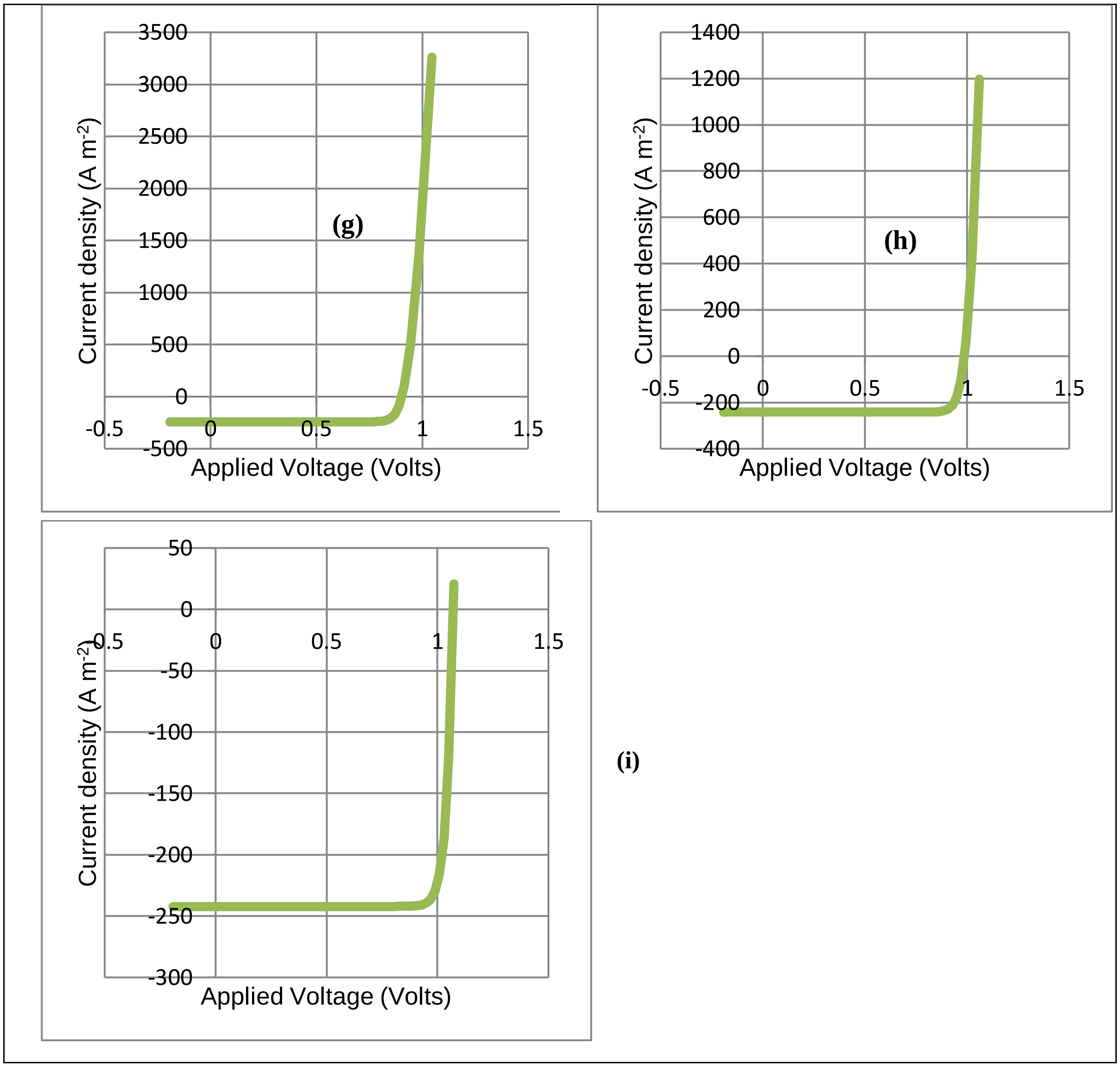

Figure 2B *Current density - Applied voltage Curves for second set of Simulations: (g)* $Bandgap = 1.51\ eV$*, (h)* $Bandgap = 1.60\ eV$ *and (i)* $Bandgap = 1.68\ eV$

S/No.	Thickness (μm)	Voc(V)	Jsc (Am^{-2})	FF	Efficiency η (%)
1.	1.0	0.6043	-235.9111	81.0941	11.560
2.	1.1	0.6063	-237.6738	81.0776	11.683
3.	1.2	0.6084	-237.4576	81.2082	11.733
4.	1.3	0.6103	-236.9925	81.3436	11.765
5.	1.4	0.6123	-238.1428	81.4317	11.874
6.	1.5	0.6144	-239.1517	81.4277	11.964
7.	1.6	0.6171	-242.2215	81.4352	12.172
8.	1.7	0.6185	-238.6963	81.4433	12.024
9.	1.8	0.6199	-235.4440	81.4323	11.885
10.	1.9	0.6208	-234.4603	81.4982	11.861
11.	2.0	0.6215	-233.4107	81.5557	11.832

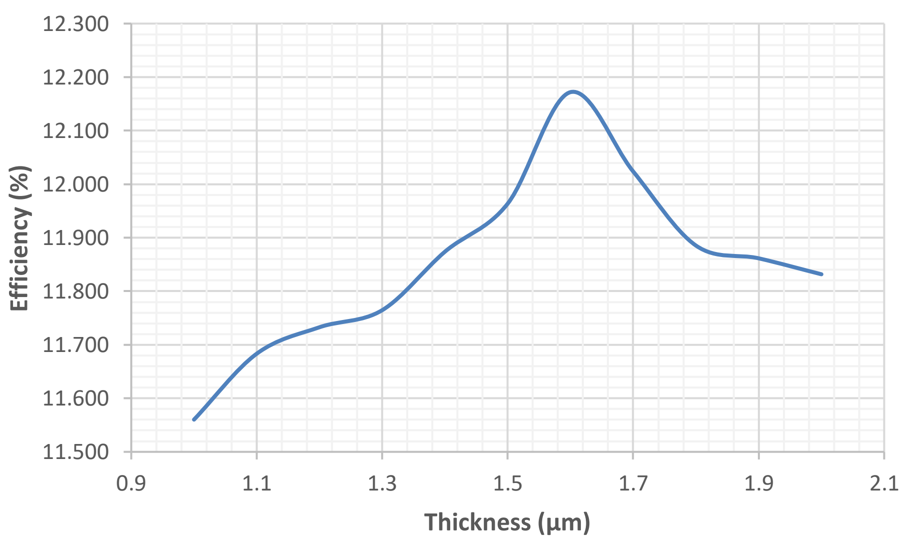

Figure 3 Graph of Efficiency against Thickness

The data in Table 1 clearly shows that the fill factor values show fluctuations as the thickness of the CIGS layer increases. The values are within a narrow range (0.4781), this shows that changes in thickness a little impact on the Fill Factor. As the thickness of the CIGS absorber layer increases from 1.0 μm to 1.5 μm, the efficiency of the solar cell also increases steadily (see Figure 3). This is obvious from the efficiency values increasing from 11.560% to 11.964%, reaching a peak of 12.172% at a thickness of 1.6 µm. Beyond the optimal efficiency value, as the thickness continues to increase from 1.7 µm to 2.0 µm, the efficiency of the solar cell starts to decline gradually, from 12.024% to 11.832%.

Thicker absorber layers absorb more light, this increases the number of photons available for the generation electron-hole pairs. However, after a certain threshold, the additional thickness leads to excessive light absorption and increased recombination, negatively impacting efficiency [19]. At the threshold point the benefits of increased light absorption and electron-hole pair generation from a thicker absorber layer start to diminish due to various factors such as excessive absorption, increased recombination, strain and defects [20], charge transport, and optical confinement.

These observations indicates that while a thicker absorber layer initially increases efficiency due to enhanced light absorption, there is an optimal thickness range where other factors, such as carrier collection efficiency and recombination losses, balance out. Beyond this range, the negative impact of increased recombination and optical losses outweighs the benefits of increased absorption, leading to decreasing efficiency.

Table 1 Bandgap, Voc, Jsc, FF and Efficiency obtained from the second set of

S/No.	Bandgap (eV)	Voc(V)	Jsc (Am^{-2})	FF	Efficiency (%)
1.	1.01	0.4261	-242.1805	75.9687	7.839
2.	1.09	0.5100	-242.2005	78.8587	9.741
3.	1.18	0.5945	-242.2175	80.9971	11.664
4.	1.26	0.6784	-242.2320	82.6287	13.579
5.	1.35	0.7620	-242.2449	84.1387	15.532
6.	1.43	0.8452	-242.2565	85.4329	17.493
7.	1.51	0.9290	-242.2669	86.4717	19.461
8.	1.60	1.0122	-242.2763	87.3104	21.411
9.	1.68	1.0971	-242.2851	87.9813	23.386

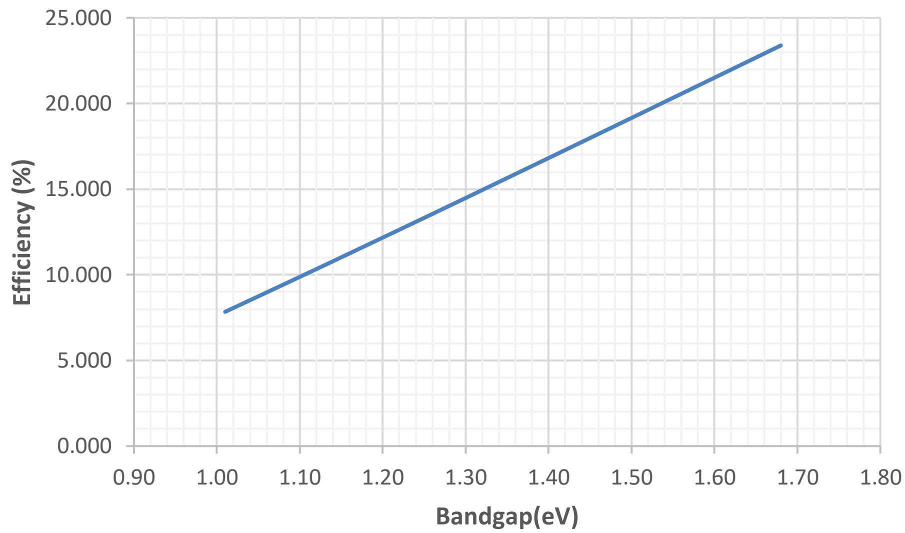

Figure 4 *Graph of Efficiency against Bandgap*

It is evident from Table 2, that the fill factor values increase as the bandgap of the CIGS layer increases. there is a positive correlation between the bandgap and the Fill Factor.

The graph in Figure 4 shows that, at the lower end of the bandgap spectrum (1.01 eV), the efficiency of the solar cell is relatively low (7.8394%). This can be attributed to the fact that the bandgap is too small to efficiently capture higher-energy photons. As the bandgap increases, there is a clear upward trend in efficiency. For example, at a bandgap of 1.680 eV, the efficiency reaches its highest value of 23.3858%.

The data suggests that there is an optimal range of bandgap values (between 1.261 eV and 1.596 eV) where efficiency increases notably. This range appears to strike a balance between allowing the absorption of a sufficient range of photon energies while minimizing the impact of excessive energy losses through thermalization [21] and non-radiative recombination. Larger bandgap allows materials to absorb higher-energy photons. but, when the bandgap becomes too large, the material might become less efficient at absorbing lower-energy photons, leading to reduced overall efficiency [22].

5 Conclusion

In conclusion, this study investigated the influence of CIGS solar cell efficiency in relation to absorber layer thickness and bandgap. The investigation, facilitated by the General-Purpose Photovoltaic Device Model (GPVDM). It was observed that as the thickness of the absorber layer (CIGS) increases, the efficiency of device increases up to when the thickness reaches 1.6 µm. When the thickness exceeds 1.6 µm the efficiency drops. At the optimal thickness of 1.6 µm the devices were found to have power conversion efficiency up to 12.172%. On other hand the fill factor fluctuates as the thickness of the CIGS layer increases. The study shows that as the bandgap increases, there is a clear upward trend in efficiency and the optima bandgap value is 1.680 eV, at this value the efficiency was found to be 23.3858%. there is a positive correlation between the bandgap and the fill factor because fill factor values increase as the bandgap of the CIGS layer increases.

References

[1] SZE, S.M. and M.K. LEE, *Semiconductor Devices: Physics and Technology* 2012: John Wiley & Sons, Inc.

[2] Nerat, M., Copper–indium–gallium–selenide (CIGS) solar cells with localized back contacts for achieving high performance. Solar energy materials and solar cells, 2012. **104**: p. 152-158.

[3] Ramanujam, J. and U.P. Singh, *Copper indium gallium selenide based solar cells–a review.* Energy & Environmental Science, 2017. **10**(6): p. 1306-1319.

[4] Andreas, B., et al., PHOTOVOLTAICS REPORT-Prepared by Fraunhofer Institute for Solar Energy Systems, ISE with support of PSE Projects GmbH. 21 February 2023, Fraunhofer Institute for Solar Energy Systems.

[5] Ramanathan, K., et al., *Properties of 19.2% efficiency ZnO/CdS/CuInGaSe$_2$ thin-film solar cells.* Progress in Photovoltaics: research and applications, 2003. **11**(4): p. 225-230.

[6] Repins, I., et al., *19· 9%-efficient ZnO/CdS/CuInGaSe$_2$ solar cell with 81· 2% fill factor.* Progress in Photovoltaics: Research and applications, 2008. **16**(3): p. 235-239.

[7] HIZIA, A., The effect of permittivity on CIGS solar cells. 2019.

[8] Kaneshiro, J., et al., *Advances in copper-chalcopyrite thin films for solar energy conversion.* Solar Energy Materials and Solar Cells, 2010. **94**(1): p. 12-16.

[9] Belghachi, A. and N. Limam, *Effect of the absorber layer band-gap on CIGS solar cell.* Chinese Journal of Physics, 2017. **55**(4): p. 1127-1134.

[10] Morales-Acevedo, A., *A simple model of graded band-gap CuInGaSe2 solar cells.* Energy Procedia, 2010. **2**(1): p. 169-176.

[11] Touafek, N. and R. Mahamadi, *Back surface recombination effect on the ultra-thin CIGS solar cells by SCAPS.* International Journal of Renewable Energy Research, 2014. **4**(4): p. 958-964.

[12] Xu, M., et al., A study on the optics of copper indium gallium (di) selenide (CIGS) solar cells with ultra-thin absorber layers. Optics express, 2014. **22**(102): p. A425-A437.

[13] Khoshsirat, N., et al., Analysis of absorber layer properties effect on CIGS solar cell performance using SCAPS. Optik, 2015. **126**(7-8): p. 681-686.

[14] Ikegami, T., et al., Estimation of equivalent circuit parameters of PV module and its application to optimal operation of PV system. Solar energy materials and solar cells, 2001. **67**(1-4): p. 389-395.

[15] Nelson, J., *Imperial College Press.* The physics of solar cells, 2003.

[16] Bimenyimana, S., G.N.O. Asemota, and L. Lingling, Output Power Prediction of Photovoltaic Module Using Nonlinear Autoregressive Neural Network. power, 2014. **31**: p. 12.

[17] MacKenzie, R.C., *Gpvdm manual.* 2016.

[18] MacKenzie, R.C., et al., *Modeling nongeminate recombination in P3HT: PCBM solar cells.* The Journal of Physical Chemistry C, 2011. **115**(19): p. 9806-9813.

[19] Guo, B., et al., *Understanding excitonic behavior in light absorption and recombination process.* The Journal of Physical Chemistry C, 2020. **124**(47): p. 26076-26082.

[20] Leijtens, T., et al., Carrier trapping and recombination: the role of defect physics in enhancing the open circuit voltage of metal halide perovskite solar cells. Energy & Environmental Science, 2016. **9**(11): p. 3472-3481.

[21] Eperon, G.E., M.T. Hörantner, and H.J. Snaith, *Metal halide perovskite tandem and multiple-junction photovoltaics.* Nature Reviews Chemistry, 2017. **1**(12): p. 0095.

[22] *SOLAR CELL CENTRAL-P/N Junctions and Band Gaps*. 2011 [cited 2023 27/08/2023]; Available from: http://solarcellcentral.com/junction_page.html